Eur. Phys. J. B **58**, 197–206 (2007)
DOI: 10.1140/epjb/e2007-00215-3

THE EUROPEAN PHYSICAL JOURNAL B

Phase transition in a mixture of adaptive cruise control vehicles and manual vehicles

R. Jiang[1,a], M.-B. Hu[1], B. Jia[2], R. Wang[3], and Q.-S. Wu[1]

[1] School of Engineering Science, University of Science and technology of China, Hefei 230026, China
[2] School of Traffic and Transportation, Beijing Jiaotong University, Beijing 100044, P.R. China
[3] Institute of Information Sciences and Technology, Massey University, New Zealand

Received 9 February 2007 / Received in final form 25 June 2007
Published online 10 August 2007

Abstract. In this paper, we have investigated the effects of adaptive cruise control (ACC) vehicles in a mixture with manually-controlled (manual) vehicles. The manual vehicles are simulated by using the modified comfortable driving model, which can describe synchronized traffic flow. The phase transition probabilities from free flow to synchronized flow and from synchronized flow to jams are studied. The impact of ACC vehicles on the flow rates in free flow and synchronized flow and on the propagation velocity of the downstream front of jams are investigated. The dependence of microscopic properties of traffic flow, including the spatiotemporal patterns and the velocity distribution, is explored. Our results are expected to be useful for developing ACC systems.

PACS. 45.70.Vn Granular models of complex systems; traffic flow – 89.40.-a Transportation – 02.60.Cb Numerical simulation; solution of equations

1 Introduction

Recently, research on vehicles equipped with adaptive cruise control (ACC) systems has attracted the interest from both physicists and engineers [1–26]. ACC is a driver assistance system designed to provide more convenience and comfort to a driver. An ACC-equipped vehicle can detect the presence of a preceding vehicle and measures the distance (range) as well as the relative speed (range rate) by using a forward-looking sensor. It automatically adjusts the vehicle speed to keep a proper range when a preceding vehicle is detected. Obviously, ACC vehicles will have some impact on the characteristics of traffic flow, including highway safety, efficiency and capacity, because of their different behavior compared with human drivers. Therefore, before ACC vehicles are deployed on a large scale, their effects on the traffic flow characteristics need to be carefully investigated.

We briefly summarize research assessing the impact of the increasing proportion of ACC vehicles as follows. The range policy of ACC vehicles has been studied in references [9–11]. The impact of ACC vehicles on highway safety has been investigated in references [12–14]. VanderWerf et al. specifically considered the effects of ACC vehicles on highway capacity [21]. Ioannou and Stefanovic [19] analyzed mixed traffic, considering the effects of unwanted cut-ins due to larger gaps in front of ACC vehicles. Zhang and Ioannou [20] concluded that there were environmental benefits due to reduced exhaust emissions. The effects of ACC vehicles on traffic flow stability are widely studied [13–18]. Treiber et al. [23] reported that if 20% of vehicles were equipped with ACC, nearly all of the congestion could be eliminated. Even for only 10%, they found that the additional travel time due to traffic jams was reduced by more than 80%. Kerner [22] found that ACC vehicles suppress wide moving jams and thus promote stability. However, he also suggested that in some cases ACC vehicles could induce congestion at bottlenecks. Davis [24] showed that ACC vehicles can suppress wide moving jams by making the flow string stable. He also proposed a cooperative merging for ACC vehicles to improve throughput and increase distances travelled in a fixed time [25]. However, to our knowledge, the effects of ACC vehicles on phase transitions in the traffic flow of a mixture of ACC vehicles and manual vehicles have not been studied.

In the literature mentioned above, ACC vehicles are modelled by using either car-following models or macroscopic models. Comparing with car-following models or macroscopic models, cellular automata (CA) models are conceptually simpler and can be easily implemented on computers for numerical investigations. Therefore, they have developed very quickly since the birth of the Nagel-Schreckenberg model.

[a] e-mail: rjiang@ustc.edu.cn

In a recent paper, we have proposed a CA model for ACC vehicles [26]. The effect of mixing ACC vehicles with manually controlled (manual) vehicles modelled by the Nagel-Schreckenberg model is explored. It is found that with the introduction of ACC vehicles, the jam can be suppressed.

However, the Nagel-Schreckenberg model is only a minimal model and it cannot describe some observed traffic phenomenon such as metastable state, capacity drop, and synchronized flow. Therefore, in this paper, the mixture of ACC vehicles with manual vehicles is investigated by using a more realistic CA model. To this end, the modified comfortable driving model, which can describe the first order phase transition from free flow to synchronized flow is used to simulate manual vehicles. The phase transition behavior will be studied in a mixture of ACC vehicles and manual vehicles in detail.

In the next section, the models for simulating ACC vehicles and manual vehicles are briefly reviewed. The simulation results are presented and analyzed in Section 3. The conclusions are given in Section 4.

2 CA models for ACC vehicles and manual vehicles

In this section, we briefly review the CA models for modelling ACC vehicles and manual vehicles. In CA models, a road is divided into cells. Each cell is either empty or occupied by a vehicle. The vehicles move with an integer velocity $1, 2, \cdots, v_{max}$ with v_{max} the maximum velocity of vehicles.

The model for ACC vehicles is recently presented in reference [26], in which a constant time headway (CTH) policy is adopted. The parallel updating rules of the model are as follows.

(i) Acceleration or deceleration: $v_n(t+1) = \min(v_{max}, \lceil d_n(t)/T \rceil)$;
(ii) randomization: $v_n(t+1) = \max(0, v_n(t+1)-1)$ with probability $p = \lceil d_n(t)/T \rceil - d_n(t)/T$ for $d_n(t)/T < v_{max}$ and $p = 0$ for $d_n(t)/T \geq v_{max}$. Note $v_n(t+1)$ on the right hand side of the equation refers to that determined in the previous step in this and following equations;
(iii) motion of a vehicle: $x_n(t+1) = x_n(t) + v_n(t+1)$.

Here v_n is the velocity of vehicle n, $d_n = x_{n+1} - x_n - L$ is the inter-vehicle distance, L is the vehicle length, x_n is the position of vehicle n, and vehicle $n+1$ precedes vehicle n. T is the time headway preferred by ACC vehicles. $\lceil x \rceil$ denotes the minimum integer that is not smaller than x.

The model for manual vehicles is presented in references [27–29]. The parallel updating rules of the model are as follows.

1. Determination of the randomization parameter $p_n(t+1)$:
$$p_n(t+1) = p(v_n(t), b_{n+1}(t), t_{h,n}, t_{s,n})$$
2. Acceleration:
if $((b_{n+1}(t) = 0$ or $t_{h,n} \geq t_{s,n})$ and $(v_n(t) > 0))$ then: $v_n(t+1) = \min(v_n(t)+2, v_{max})$ else if $(v_n(t) = 0)$ then: $v_n(t+1) = \min(v_n(t)+1, v_{max})$ else: $v_n(t+1) = v_n(t)$
3. Braking rule:
$v_n(t+1) = \min(d_n^{eff}, v_n(t+1))$
4. Randomization and braking:
if $(rand() < p_n(t+1))$ then: $v_n(t+1) = \max(v_n(t+1)-1, 0)$
5. The determination of $b_n(t+1)$:
if $((v_n(t+1) > v_n(t))$ or $(v_n(t+1) \geq v_c$ and $t_{f,n} > t_{c1}))$ then: $b_n(t+1) = 0$
else if $(v_n(t+1) < v_n(t))$ then: $b_n(t+1) = 1$
else $(v_n(t+1) = v_n(t))$ then: $b_n(t+1) = b_n(t)$
6. The determination of $t_{st,n}$:
if $v_n(t+1) = 0$ then: $t_{st,n} = t_{st,n} + 1$
if $v_n(t+1) > 0$ then: $t_{st,n} = 0$
7. The determination of $t_{f,n}$:
if $v_n(t+1) \geq v_c$ then: $t_{f,n} = t_{f,n} + 1$
if $v_n(t+1) < v_c$ then: $t_{f,n} = 0$
8. Motion of a vehicle:
$x_n(t+1) = x_n(t) + v_n(t+1)$.

Here b_n is the status of the brake light (on(off)$\rightarrow$ $b_n = 1(0)$). The two times $t_{h,n} = d_n/v_n(t)$ and $t_{s,n} = \min(v_n(t), h)$, where h determines the range of interaction with the brake light, are introduced to compare the time $t_{h,n}$ needed to reach the position of the leading vehicle with a velocity dependent interaction horizon $t_{s,n}$. The effective distance is $d_n^{eff} = d_n + \max(v_{anti} - gap_{safety}, 0)$, where $v_{anti} = \min(d_{n+1}, v_{n+1})$ is the expected velocity of the preceding vehicle in the next time step and gap_{safety} controls the effectiveness of the anticipation. $rand()$ is a random number between 0 and 1, $t_{st,n}$ denotes the time that the car n stops, $t_{f,n}$ denotes the time that car n is in the state $v_n \geq v_c$. The randomization parameter p is defined:

$$p(v_n(t), b_{n+1}(t), t_{h,n}, t_{s,n}) = \begin{cases} p_b : \text{if } b_{n+1} = 1 \text{and } t_{h,n} < t_{s,n} \\ p_0 : \text{if } v_n = 0 \text{ and } t_{st,n} \geq t_c \\ p_d : \text{in all other cases.} \end{cases}$$

Here v_c, t_{c1}, and t_c are parameters.

3 Simulation results

In this section, the simulation results are presented and analyzed. In the simulations, the parameter values are $t_c = 9$, $t_{c1} = 30$, $v_c = 18$, $v_{max} = 20$, $p_d = 0.25$, $p_b = 0.94$, $p_0 = 0.5$, $h = 6$ and $gap_{safety} = 7$. Each cell corresponds to 1.5 m and a vehicle has a length of five cells. One time step corresponds to 1 s. Periodic boundary conditions are adopted in the simulations and the road length is set to $L_r = 10000$.

Figure 1 shows the fundamental diagram of 100% ACC vehicles (i.e., $R = 1$) at different values of T. Here R denotes the ratio of ACC vehicles. A triangular curve of flow rate versus density is reproduced as the CTH policy is adopted. With the increase of parameter T, both

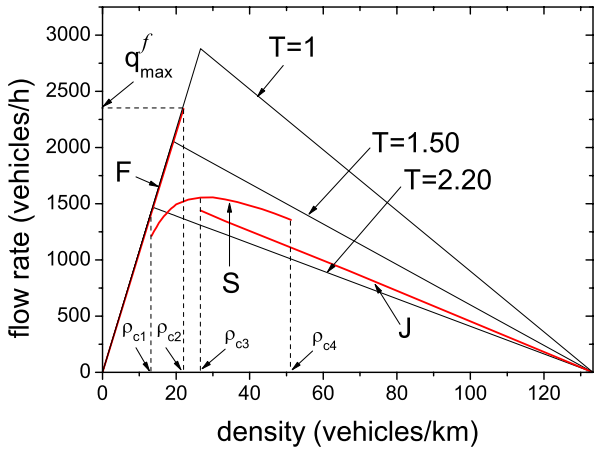

Fig. 1. Fundamental diagrams of 100% ACC vehicles at different values of T (black lines) and of 100% manual vehicles (red lines). F, S and J mean the free flow branch, synchronized flow branch, and jam branch of 100% manual vehicles, respectively.

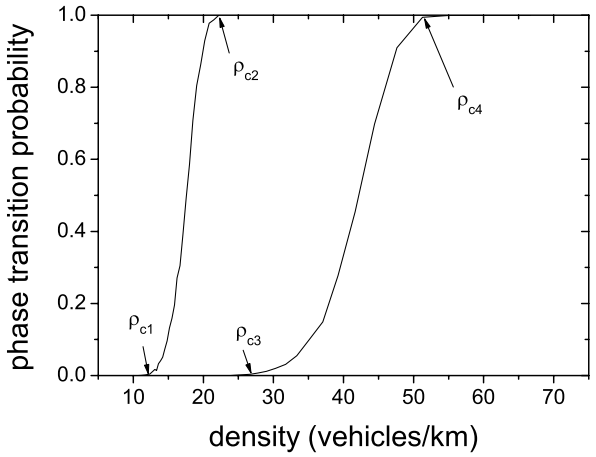

Fig. 2. Phase transition probabilities from free flow to synchronized flow (left curve) and from synchronized flow to jams (right curve) for 100% manual vehicles.

the maximum flow rate and the corresponding density decrease.

The fundamental diagram of 100% manual vehicles ($R = 0$) is also shown in Figure 1. Initially, the vehicles are homogeneously distributed on the road. We focus on the probability of the phase transition (see Ref. [30] for details of phase transition probability)[1]. To this end, a large number of runs of the same duration $T_0 = 6000$ have been studied for a given density. For each run it was checked whether the phase transition (either from free flow to synchronized flow or from synchronized flow to jam) occurred within the given time interval T_0 or not. We record the number of realizations n_P where the phase transition had occurred. Then $P \approx n_P/N_P$ is the approximate probability that the phase transition occurs during the time interval T_0 at the given density. Here $N_P = 1000$ is the number of all realizations.

The simulations show there are four critical densities. When the density is smaller than ρ_{c1}, the probability of the phase transition from free flow to synchronized flow is zero; when the density is larger than ρ_{c2}, the probability of the phase transition from free flow to synchronized flow is one; when $\rho_{c1} < \rho < \rho_{c2}$, the phase transition probability is shown in Figure 2. We denote the maximum flow rate corresponding to ρ_{c2} as q^f_{max}. Similarly, when the density is smaller than ρ_{c3}, the probability of the phase transition from synchronized flow to jam is zero; when the density is larger than ρ_{c4}, the probability of the phase transition from synchronized flow to jam is one; When the density $\rho_{c3} < \rho < \rho_{c4}$, the phase transition probability is also shown in Figure 2. In Figure 3, the typical spatiotemporal patterns of the phase transition processes are shown.

Comparing the fundamental diagrams of 100% ACC vehicles and 100% manual vehicles, one can see that the maximum flow rate corresponding to $T = 1.0$ is larger than q^f_{max}, and the maximum flow rate corresponding to $T = 1.5$ is smaller than q^f_{max}. In addition, the congested branches corresponding to $T = 1.0$ and $T = 1.5$ are above the congested branch of manual vehicles, and the congested branch of ACC vehicles is below that of manual vehicles for $T = 2.20$. Next we study the mixture of manual vehicles and ACC vehicles with $T = 1.0, 1.5$ and 2.2 respectively.

3.1 Effects of ACC vehicles on F → S

In this section, we focus on the effects of ACC vehicles on the phase transition from free flow to synchronized flow in a mixture of ACC vehicles and manual vehicles. Figure 4 shows the phase transition probability curve under different values of T and R. It can be seen that:

(i) For $T = 1.0$, ACC vehicles move deterministically. One can see that with the introduction of ACC vehicles, phase transition probability curve moves right. This means that phase transition occurs more difficult, i.e., ACC vehicles could enhance the stability of free flow.

(ii) When $T > 1$, ACC vehicles could not move deterministically in the CA model. As a result, velocity fluctuation appears in traffic flow composed of 100% ACC vehicles. Figure 5 shows the velocity variance of ACC vehicles in a stationary state. One can see that the velocity fluctuation is extremely strong when $0 < T - 1 \ll 1$. Our simulations also show that when $0 < T - 1 \ll 1$, the velocity $v_{ACC} = 17 < v_c$ could be observed for an ACC vehicle that follows a platoon of free moving manual vehicles.
This is an artificial effect of the model. As a result, the CA model of ACC vehicles is not suitable for evaluating phase transition in mixed traffic at the parameter range $0 < T - 1 \ll 1$: the fluctuation will weaken the

[1] Note the type of phase transition from free flow to synchronized flow and from synchronized flow to jams is spontaneous, instead of the deterministic type that occurs near an on-ramp or other bottleneck.

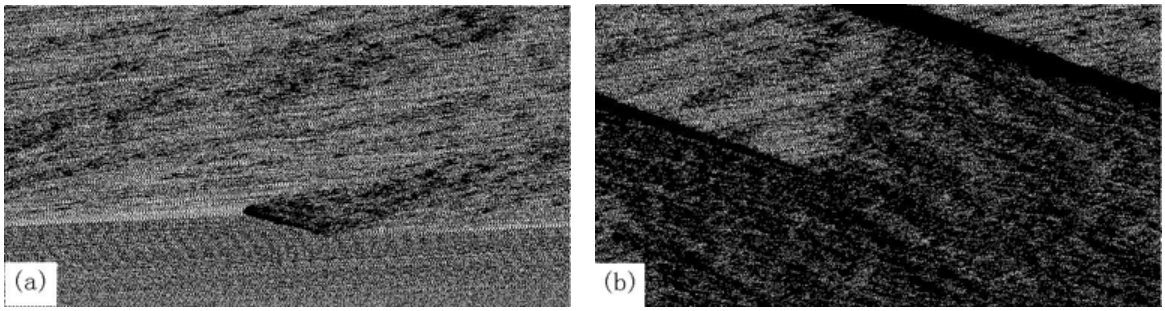

Fig. 3. Typical spatiotemporal patterns of the phase transition processes (a) from free flow to synchronized flow and (b) from synchronized flow to jams for 100% manual vehicles. In (a) $\rho = 20.2$ vehicles/km (corresponding to headway 49.5 m); (b) $\rho = 37.0$ vehicles/km (corresponding to headway 27 m).

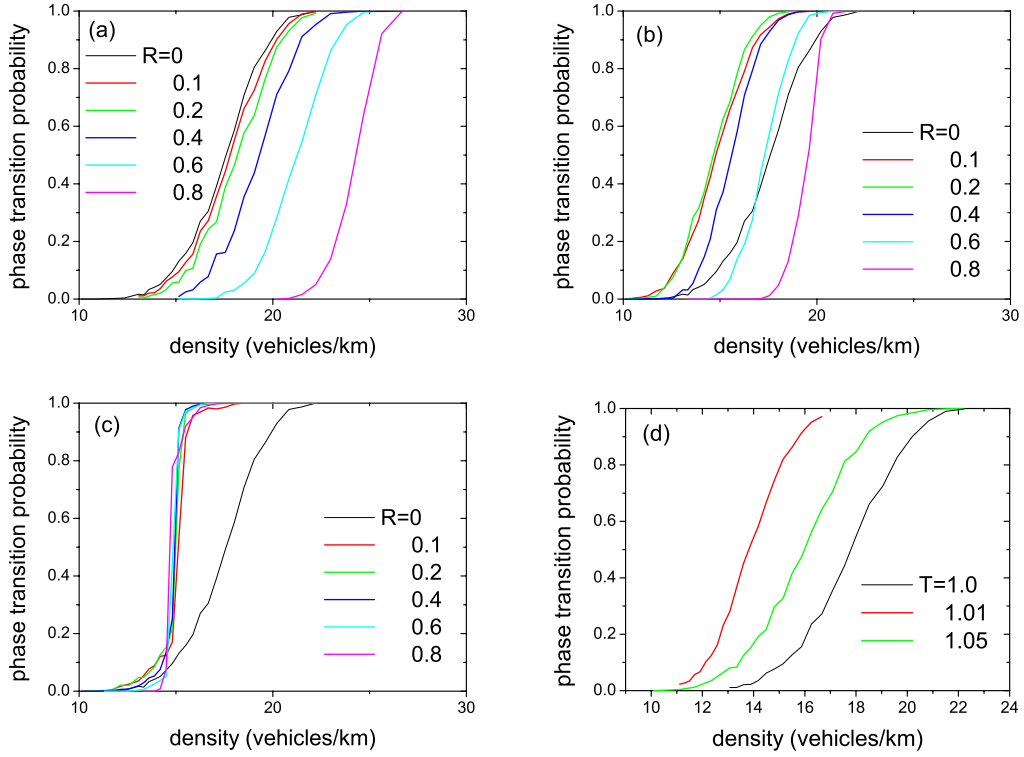

Fig. 4. Phase transition probability from free flow to synchronized flow for a mixture of ACC vehicles and manual vehicles. (a) $T = 1.0$; (b) $T = 1.5$; (c) $T = 2.20$. (d) compares the phase transition probability of $T = 1.0, 1.01$ and 1.05 at ratio $R = 0.1$.

traffic flow stability. This is supported by the simulation results shown in Figure 4d. One can see that even T slightly deviates from 1, the phase transition probability curve moves left remarkably. The curve of $T = 1.01$ is on the left of that of $T = 1.05$, which further demonstrates the influence of the intrinsic fluctuation of the CA model.

In order to properly evaluate mixed traffic flow at the parameter range $0 < T - 1 \ll 1$, we need to propose a CA model for ACC vehicles, in which the velocity fluctuation is weak. This will be further studied in our future work.

(iii) For $T = 1.50$, Figure 5 shows the velocity fluctuation is weak. Therefore, the CA model of ACC vehicles could be used for the evaluation. The simulations show that when R is small, the phase transition probability curve moves left compared with the curve of $R = 0$. This means that the phase transition occurs more easily. When the ratio of ACC vehicles is large (e.g., $R > 0.2$), the probability curve moves towards the right with the increase of R.

Comparing Figures 4a and 4b, one can see that the curves of $T = 1.50$ are on the left of that corresponding to $T = 1.0$ at any ACC vehicle ratio. This means that the phase transition occurs more easily if T increases. Furthermore, one can see that with the increase of T and/or R, the probability curve becomes steeper, which means that the metastable density range corresponding to the transition from free flow to synchronized flow shrinks.

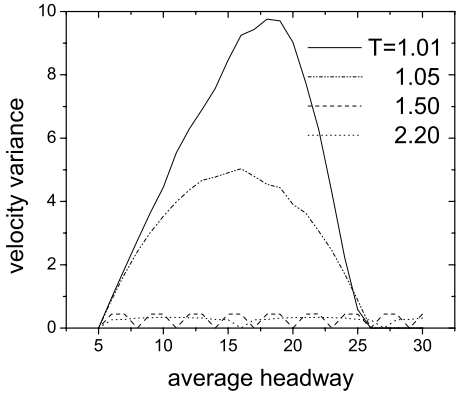

Fig. 5. Velocity variance in traffic flow of 100% ACC vehicles on a circuit road. Initially, the vehicles are homogeneously distributed on the road. One can see that the velocity fluctuation is extremely strong when $0 < T - 1 \ll 1$. This is an artificial effect of the model and is not consistent with the properties of a real ACC vehicle.

(iv) For $T = 2.20$, the results are quite different. One can see that the probability curves are very steep. Moreover, they only slightly depend on R. These curves are on the left of that corresponding to $R = 0$, which means that a phase transition occurs more easily.

The dependence of the phase transition curve on the parameters R and T might be relevant to the following effects. (1) In the free flow, the headway of ACC vehicles is $v_{max}T$ because ACC vehicles move with the maximum velocity. The total headway of ACC vehicle is, therefore, $NRv_{max}T$. Here NR is the number of ACC vehicles. This leads to the effective headway for manual vehicles $h_{\text{eff}} = \frac{L_r - NRv_{max}T}{N(1-R)}$, which may be different from the average headway $h = \frac{L_r}{N}$. As a result, the stability is enhanced when $h_{\text{eff}} > h$ and is weakened when $h_{\text{eff}} < h$. (2) With the increase of ACC vehicle ratio, the chance that a large platoon of manual vehicles could exist decreases. This will enhance the stability. (3) An ACC vehicle will change the moving behavior of the manual vehicle that follows it, because the velocity of the ACC vehicle $v_{\text{ACC}} = d_{n+1}/T$ might be much smaller than the expected velocity $v_{anti} = \min(d_{n+1}, v_{n+1})$ of the manual vehicle, especially for a large T. Therefore, the collision will happen if the expected velocity of a manual vehicle, which follows an ACC vehicle, remains unchanged. In our simulations, the expected velocity is changed by using $v_{anti} = \min(d_{n+1}/T, v_{n+1})$. Obviously, this will weaken the stability if $T > 1$.

3.2 Effect of ACC vehicles on F → J

In this subsection, we focus on the effects of ACC vehicles on the phase transition from synchronized flow to jam. Figure 6 shows the phase transition probability curve under different values of T and R. It can be seen that

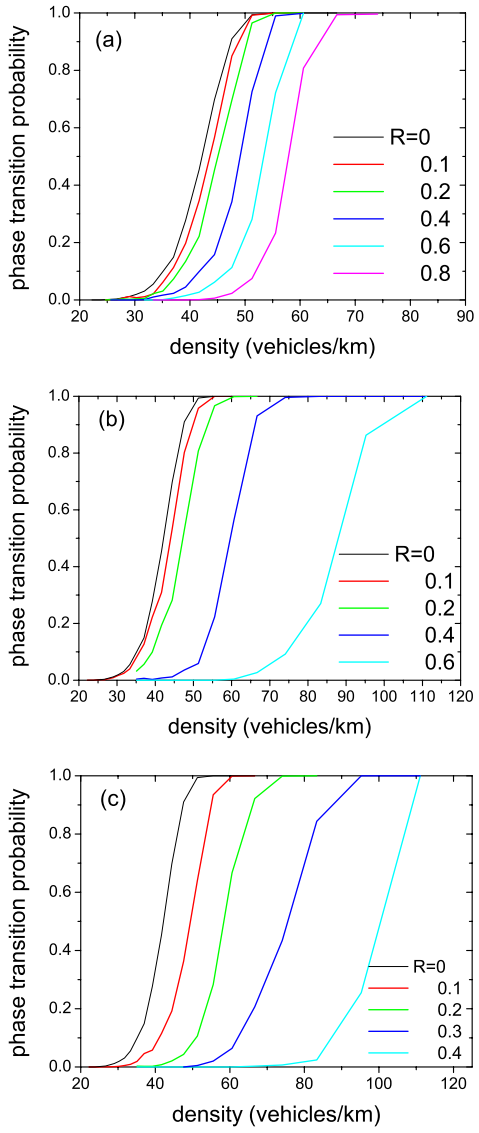

Fig. 6. Phase transition probability from synchronized flow to jams for a mixture of ACC vehicles and manual vehicles. (a) $T = 1.0$; (b) $T = 1.5$; (c) $T = 2.20$.

(i) For $T = 1.0$: With the increase of R, the probability curve shifts right. This means that with the introduction of ACC vehicles, the phase transition from synchronized flow to jams more unlikely occurs. Furthermore, with the increase of R, the probability curve becomes a little flatter, which means that the metastable density range corresponding to the transition from synchronized flow to jams expands.

(ii) For $T = 1.50$ and $T = 2.20$, similar results are observed. When $T = 1.50$ and $R \gtrsim 0.8$, a jam will not spontaneously appear from synchronized flow. This is because the propagating speed of the downstream front of a jam is so large that the jam will soon dissolve even if it forms due to reasons such as car accidents. This can be seen from Figure 7. When $T = 2.20$, a

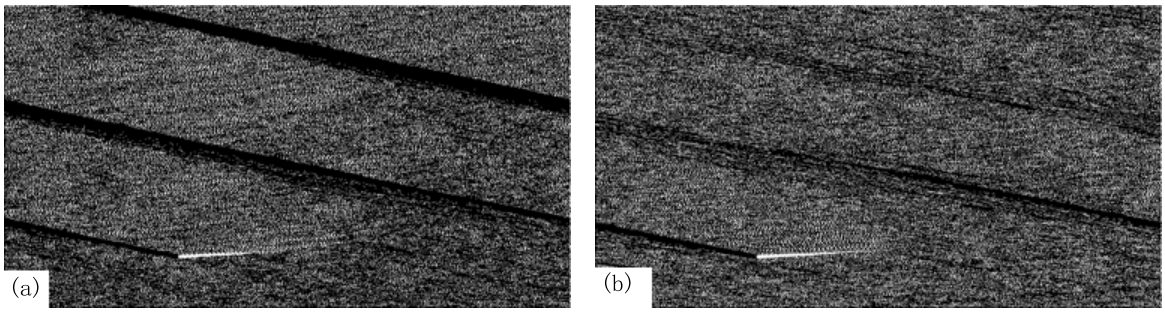

Fig. 7. Evolution of traffic jams due to reasons such as car accidents. $\rho = 33.3$ vehicles/km (corresponding to headway 30 m), $T = 1.50$. (a) $R = 0.6$ (b) $R = 0.8$. One can see that an induced jam will be maintained and widened for $R = 0.6$ but dissolved for $R = 0.8$.

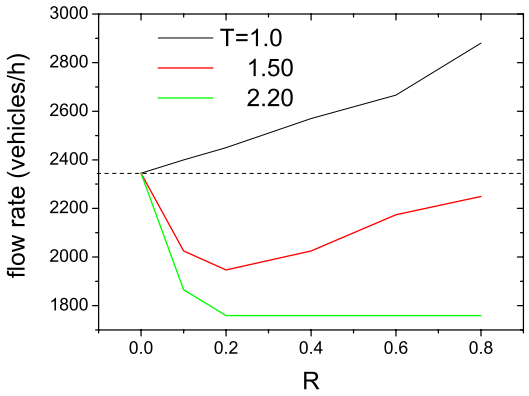

Fig. 8. q^f_{max} in a mixture of ACC vehicles and manual vehicles.

jam will not spontaneously appear from synchronized flow provided $R > 0.4$.

We have compared the probability curves of $T = 1.0$, $T = 1.50$ and $T = 2.20$, and found that the curves of $T = 2.20$ are always rightmost and the curves of $T = 1.0$ are always leftmost at any ACC vehicle ratio (not shown). This means that the phase transition more unlikely occurs if T increases. This is opposite to the effects of ACC vehicles on $F \to S$ discussed in the previous subsection.

3.3 Effects of ACC vehicles on flow rate

In this section, we discuss the effects of ACC vehicles on the flow rate in free flow, synchronized flow and jams, respectively. Our simulations show that the introduction of ACC vehicles essentially does not affect the slope of the flow rate curve in free flow, because the maximum velocity of ACC vehicles is the same as that of manual vehicles. Nevertheless, the introduction of ACC vehicles will affect q^f_{max} because ρ_{c2} is different under different values of R and T. Figure 8 shows the curves of q^f_{max} versus R at different values of T. One can see that at a given R, the larger T is, the smaller q^f_{max} is. For $T = 1.0$, q^f_{max} is increasing with R; for $T = 1.50$, q^f_{max} firstly decreases and then increases with R; for $T = 2.20$, q^f_{max} firstly decreases with R, then essentially remains constant.

Furthermore, for $T = 1.50$ and $T = 2.20$, a q^f_{max} larger than that of 100% manual vehicles cannot be achieved at large R. This is because for $T = 1.50$ and $T = 2.20$, the maximum flow rate of 100% ACC vehicles is smaller than q^f_{max} of 100% manual vehicles.

Figure 9 shows the flow rate in synchronized flow under different values of R and T. For $T = 1.0$, the flow rate increases with the increase of R. Even at $R = 0.8$, the flow rate is still far below that of 100% ACC vehicles. For $T = 1.50$, the flow rate also increases with the increase of R. Nevertheless, when $R \approx 0.4$, the flow rate at large densities is approximately the same as that of 100% ACC vehicles and the flow rate at small densities still increases with R. For $T = 2.20$, the situation is quite different. It is interesting to find that the flow rate firstly slightly increases when $R = 0.1$. Then, the flow rate at large density $\rho > \rho_{cc}$ decreases with the increase of R but the flow rate at small density $\rho < \rho_{cc}$ essentially remains unchanged. The value of ρ_{cc} decreases with the increase of R. Even at $R = 0.8$, the flow rate is still notably above that of 100% ACC vehicles.

Finally, our simulations show that the introduction of ACC vehicles will affect the slope of the jam line, i.e. the propagation velocity of the downstream front of the jams. Figure 10 shows the absolute value of the jam line slope under different values of T, in which a megajam composed of 2000 vehicles is studied[2]. We let the first vehicle accelerate at time $t = 0$, and record the time t_m that the last vehicle moves. Then the slope is calculated by $15000/t_m$.

It can be seen for $T = 1.0$ and $T = 1.50$, the absolute value of the slope increases with the increase of R. Note that for $T = 1.50$, the slope increases fast when $\rho < \rho_{cv}$ but increases slowly when $\rho > \rho_{cv}$. In contrast, for $T = 2.20$, the absolute value of the slope firstly increases and then decreases with the increase of R. When the jam line is below the synchronized flow branch, jams may appear spontaneously from synchronized flow. When the jam line is above the synchronized flow branch, there

[2] A megajam is the jam, in which the gaps between vehicles are zero.

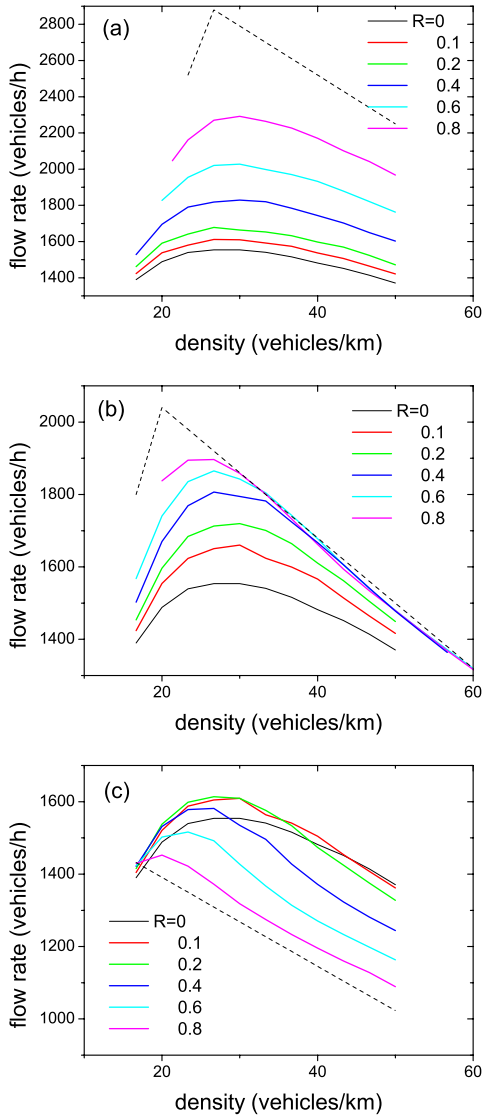

Fig. 9. Flow rate in synchronized flow under different values of R and T. The dashed line shows the flow rate of 100% ACC vehicles. (a) $T = 1.0$; (b) $T = 1.5$; (c) $T = 2.20$.

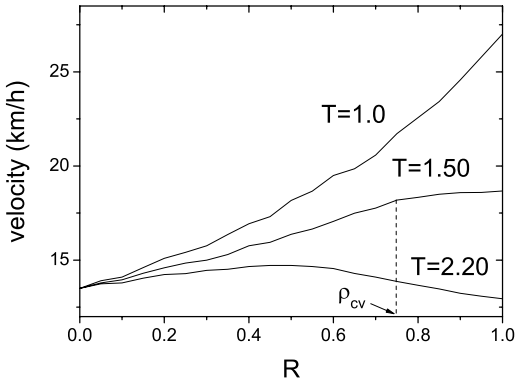

Fig. 10. Propagation velocity of the downstream front of the jams in a mixture of ACC vehicles and manual vehicles.

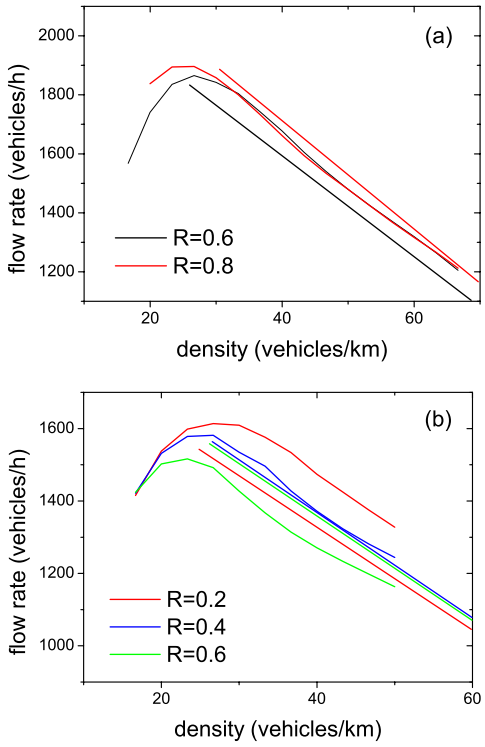

Fig. 11. The jam line and the synchronized flow branch under different values of R and T in a mixture of ACC vehicles and manual vehicles. The straight lines are the jam lines. (a) $T = 1.50$ (b) $T = 2.20$.

will be no spontaneous jam appearing from synchronized flow. Figure 11 shows the jam line and the synchronized flow branch under different values of R and T, which illustrates why jam does not spontaneously appear from synchronized flow when $R > 0.4$ for $T = 2.20$ and when $R \gtrsim 0.8$ for $T = 1.50$.

3.4 Effects of ACC vehicles on microscopic properties

In this subsection, we study the effects of ACC vehicles on spatiotemporal patterns and velocity distribution in synchronized flow. Figure 12 shows the typical spatiotemporal patterns in synchronized flow for different values of R, with the parameter $T = 1.0$ and the density $\rho = 37.04$ vehicles/km (which corresponds to headway 27 m). One can see that with the increase of R, the traffic flow gradually evolves into a mixture of free flow and synchronized flow (also see the snapshots in Fig. 13). Even at $R = 0.99$, the traffic pattern is still characterized by the mixture. However, when $R = 1$, the traffic flow is quite homogeneous (not shown).

Figure 14 shows the spatiotemporal patterns in synchronized flow with the parameter $T = 1.50$ and the density $\rho = 37.04$ vehicles/km. One can see that there also appears a mixture of free flow and synchronized flow. However, when R is large, the mixture is suppressed and the traffic flow gradually becomes homogeneous (see Fig. 15c and 15d).

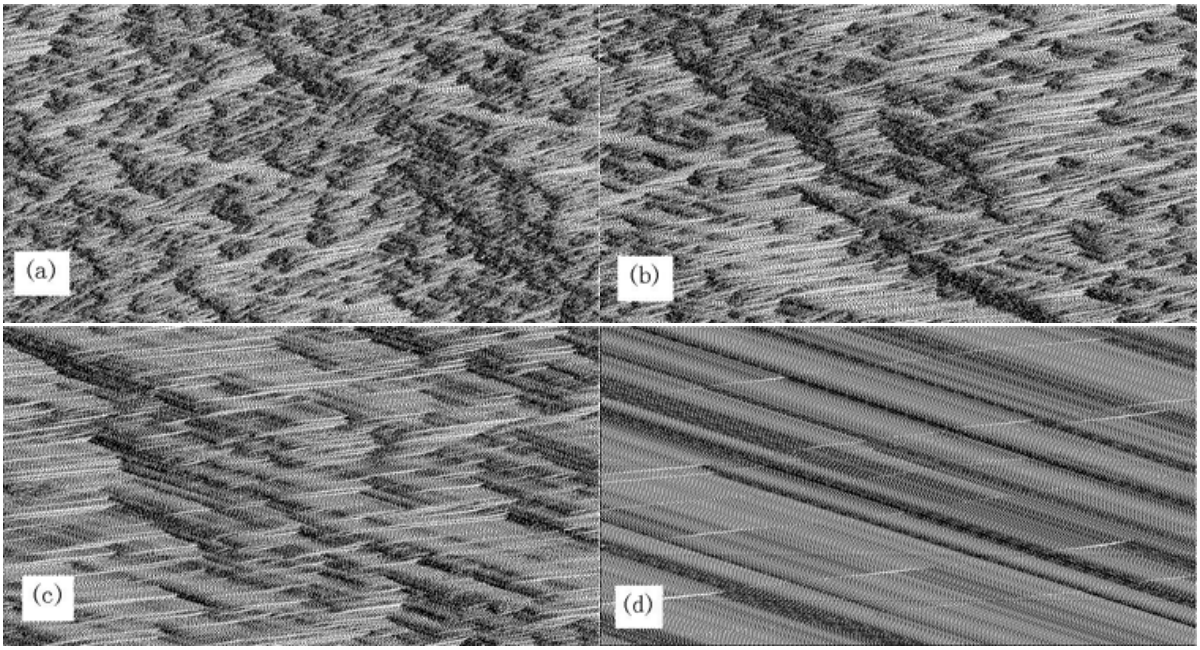

Fig. 12. Typical spatiotemporal patterns in synchronized flow for different values of R, with the parameter $T = 1.0$ and the density $\rho = 37.04$ vehicles/km. (a) $R = 0$; (b) $R = 0.4$; (c) $R = 0.8$; (d) $R = 0.99$.

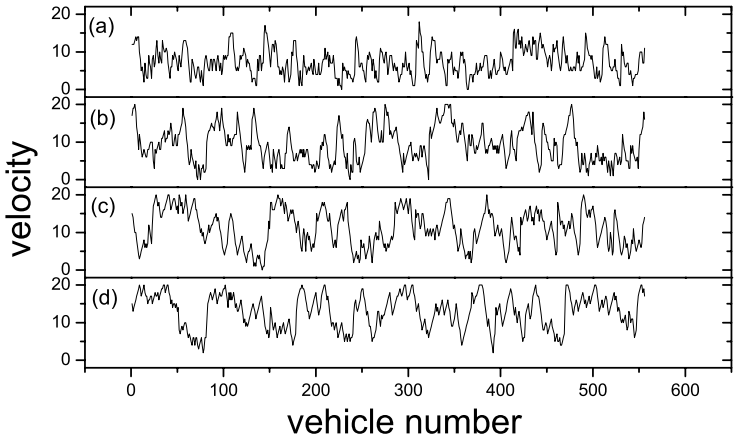

Fig. 13. Snapshots of velocity corresponding to the traffic flow in Figure 12.

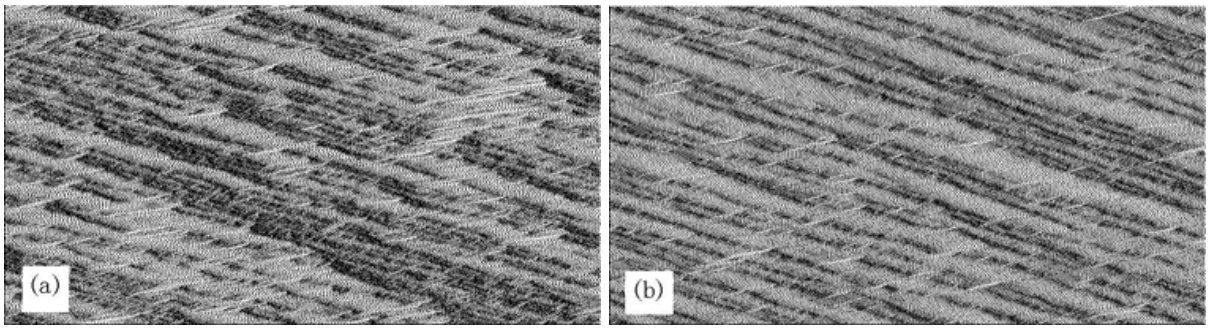

Fig. 14. Typical spatiotemporal patterns in synchronized flow at different values of R, with the parameter $T = 1.5$ and the density $\rho = 37.04$ vehicles/km. (a) $R = 0.4$; (b) $R = 0.8$.

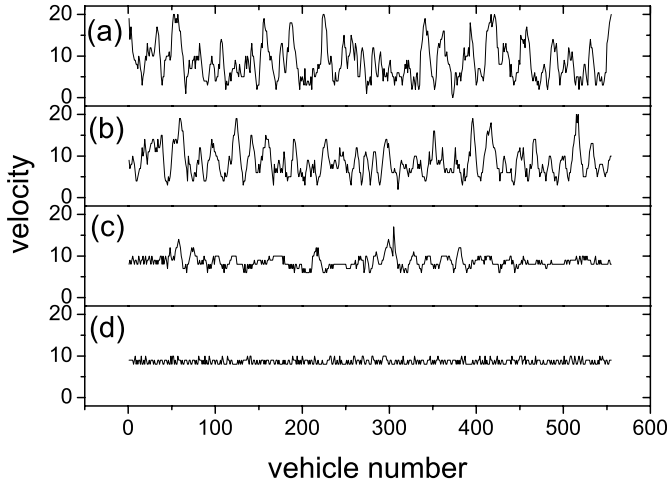

Fig. 15. Snapshots of velocity corresponding to the traffic flow in Figure 14. (a) $R = 0.4$; (b) $R = 0.8$; (c) $R = 0.99$; (d) $R = 1$.

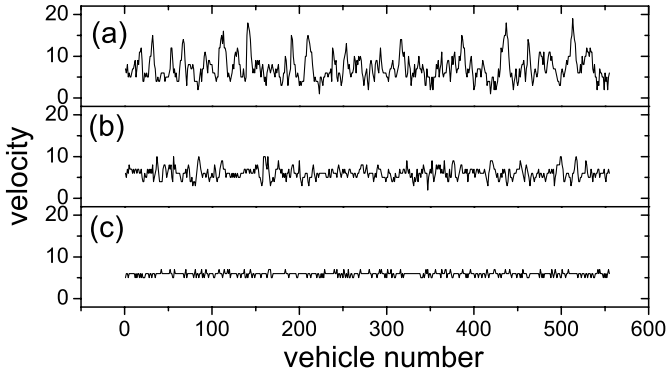

Fig. 16. Snapshots of velocity in synchronized flow for different values of R, with the parameter $T = 2.2$ and the density $\rho = 37.04$ vehicles/km. (a) $R = 0.4$; (b) $R = 0.8$; (c) $R = 1$.

Figure 16 shows the snapshots of velocity in synchronized flow when $T = 2.20$. It is found that with the increase of R, the traffic flow gradually becomes homogeneous and there is no mixture of free flow and synchronized flow.

Figure 17 shows the velocity distribution in the synchronized flow. One can see that when R is given, the distribution becomes narrower with the increase of T. This further demonstrates that if R is fixed, the traffic flow becomes more homogeneous with the increase of T.

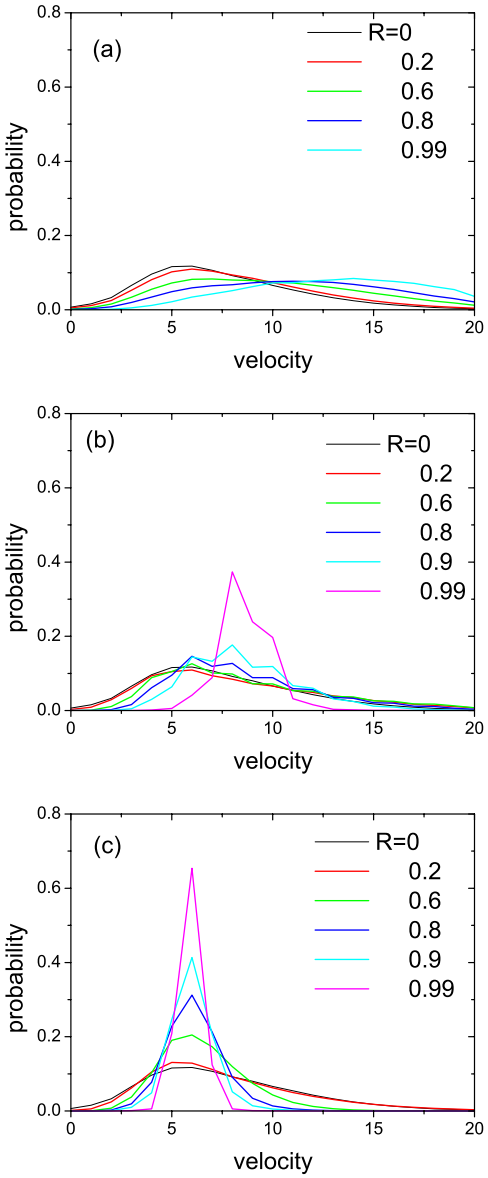

Fig. 17. Velocity distribution in the synchronized flow for different values of R, with the parameter (a) $T = 1.0$ (b) $T = 1.50$ (c) $T = 2.20$, and the density $\rho = 37.04$ vehicles/km.

4 Conclusions

Previous research on ACC vehicles has studied the impact of ACC vehicles on traffic flow stability, safety and exhaust emissions. In this paper, we mainly concentrate on the effects of ACC vehicles on the phase transition in traffic flow of a mixture of ACC and manual vehicles. Our simulations show that when the preferred time headway of ACC vehicles is small (e.g., $T = 1$), the introduction of ACC vehicles will enhance the free flow stability. However, when T is large, the introduction of ACC vehicles will reduce the phase transition threshold ρ_{c2}, and consequently reduce the maximum flow rate q^f_{max}. Different from the phase transition from free flow to synchronized flow, the introduction of ACC vehicles will generally increase the threshold from synchronized flow to jams.

Furthermore, the spatiotemporal patterns and velocity distribution of mixed ACC vehicles and manual vehicles are also studied. It is interesting to report that when T is small and the traffic is in synchronized flow, a mixture of free flow and synchronized flow will appear, even though $R = 0.99$. In other words, only several manual vehicles will seriously destroy the homogeneity of traffic flow. This is undesired and we need to find a way to suppress this phenomenon.

In our future work, this research needs to be extended to multi-lane traffic and we also need to consider the impact of various kinds of bottlenecks. Furthermore, this paper only examines the effects of ACC vehicles with the CTH policy in the framework of CA models. In future work, research on ACC vehicles with other range policies and in the framework of other kinds of models (such as car-following models) are expected.

We are grateful for an anonymous referee for his critical comments. We acknowledge the support of National Basic Research Program of China (No.2006CB705500), the National Natural Science Foundation of China (NNSFC) under Key Project No. 10532060 and Project Nos. 10404025, 70501004, 70601026, 10672160. R. Wang acknowledges the support of the ASIA:NZ Foundation Higher Education Exchange Program (2005), Massey University Research Fund (2005), and Massey University International Visitor Research Fund (2007). We are grateful to M. Gillingham for proofreading this manuscript.

References

1. B. Van Arem, C.J.G. van Driel, R. Visser, IEEE Trans. ITS **7**, 429 (2006)
2. P. Ioannou, IEEE Trans. ITS **4**, 113 (2003)
3. J. VanderWerf, S. Shladover, N. Kourjanskaia et al., Transp. Res. Rec. **1748**, 167 (2001)
4. S.E. Shladover, Transp. Res. Rec. **1727**, 154 (2000)
5. G. Marsden, M. McDonald, M. Brackstone, Transp. Res. Part C, **9**, 33 (2001)
6. P.J. Zheng, M. McDonald, Transp. Res. Part C, **13**, 421 (2005)
7. O. Gietelink, J. Ploeg, B. De Schutter et al., Veh. Sys. Dyna. **44**, 569 (2006)
8. J.S. Gu, S. Yi, K. Yi, Int. J. Auto. Tech. **7**, 619 (2006)
9. J. Zhou, H. Peng, IEEE Trans. ITS **6**, 229 (2005)
10. J.M. Wang, R. Rajamani, IEEE Trans. Veh. Tech. **53**, 1480 (2004)
11. D.H. Han, K.S. Yi, Proc. Institute Mech. Eng. Part D, **220** (D3), 321 (2006)
12. J. Wang, R. Rajamani, Proc. Institute Mech. Eng. Part D, **218** (D2), 111 (2004)
13. S. Kikuchi, N. Uno, M. Tanaka, J. Transp. Eng.-ASCE **129**, 146 (2003)
14. H. Rakha, J. Hankey, A. Patterson et al., ITS J. **6**, 225 (2001)
15. P. Fancher, H. Peng, Z. Bareket, et al., Veh. Sys. Dyna. **37**, 125 Suppl. (2002)
16. C.Y. Liang, H. Peng, JSME Int. J. Series C, **43**, 671 (2000)
17. J.G. Yi, R. Horowitz, Transp. Res., Part C, **14**, 81 (2006)
18. P.Y. Li, A. Shrivastava, Transp. Res. Part C, **10**, 275 (2002)
19. P.A. Ioannou, M. Stefanovic, IEEE Trans. ITS **6**, 79 (2005)
20. J.L. Zhang, P.A. Ioannou, IEEE Trans. ITS **7**, 92 (2006)
21. J. VanderWerf, S.E. Shladover, M.A. Miller, et al., Transp. Res. Rec. **1800**, 78 (2002)
22. B.S. Kerner, e-print `arXiv:cond-mat/0309017`.
23. M. Treiber, D. Helbing, e-print `arXiv:cond-mat/0210096`; A. Kesting, M. Treiber, M. Schoenhof, et al., e-print `arXiv:physics/0601096` (to appear in Proc. Traffic and Granular Flow '05)
24. L.C. Davis, Phys. Rev. E **69**, 066110 (2004)
25. L.C. Davis, Physica A **379**, 274 (2007)
26. R. Jiang, Q.S. Wu, Phys. Lett. A **359**, 99 (2006)
27. R. Jiang, Q.S. Wu, Eur. Phys. J. B **46**, 581 (2005)
28. R. Jiang, Q.S. Wu, J. Phys. A **37**, 8197 (2004)
29. R. Jiang, Q.S. Wu, J.Phys. A **36**, 381 (2003)
30. B.S. Kerner, S.L. Klenov, D.E. Wolf, J. Phys. A **35**, 9971 (2002)